Article

Synthesis of Face-Centered Tetragonal FePt Nanoparticles and Granular Films from Pt@FeO Core–Shell Nanoparticles

Xiaowei Teng, and Hong Yang

J. Am. Chem. Soc., **2003**, 125 (47), 14559-14563• DOI: 10.1021/ja0376700 • Publication Date (Web): 01 November 2003

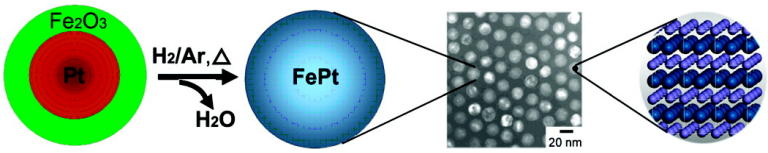

More About This Article

Additional resources and features associated with this article are available within the HTML version:

- Supporting Information
- Links to the 21 articles that cite this article, as of the time of this article download
- Access to high resolution figures
- Links to articles and content related to this article
- Copyright permission to reproduce figures and/or text from this article

View the Full Text HTML

J|A|C|S
ARTICLES
Published on Web 11/01/2003

Synthesis of Face-Centered Tetragonal FePt Nanoparticles and Granular Films from Pt@Fe_2O_3 Core−Shell Nanoparticles

Xiaowei Teng† and Hong Yang*,†,‡

Contribution from the Department of Chemical Engineering and Laboratory for Laser Energetics, 206 Gavett Hall, University of Rochester, Rochester, New York 14627-0166

Received July 31, 2003; E-mail: hongyang@che.rochester.edu

Abstract: This paper describes a new approach for making face-centered tetragonal (fct) FePt nanoparticles with a diameter of 17 nm and granular films from Pt@Fe_2O_3 core−shell nanoparticle precursors. The core−shell nanoparticles were converted to fct FePt through a reduction and alloy formation process at enhanced temperatures. The Fe and Pt elemental analysis was conducted on both individual nanoparticles and granular films using energy-dispersive X-ray (EDX) spectroscopy. Our convergent evidence from selected area electron diffraction (SAED), powder X-ray diffraction (PXRD), and EDX analysis indicates that the final products are fct FePt alloys. The fct FePt films have coercivities of 8.0−9.1 kOe at 5 K and 7.0 kOe at 300 K measured by a SQUID magnetometer. These values depend on the conversion temperatures of Pt@Fe_2O_3 nanoparticles. Unlike the previously synthesized disordered face-centered cubic (fcc) FePt nanoparticles with diameters of 4−6 nm (Sun, S. H.; Murray, C. B.; Weller, D.; Folks, L.; Moser, A. *Science* **2000**, *287*, 1989), the FePt nanoparticles presented in this work not only possess the preferred fct phase but also are in a size range that is expected to be ferromagnetic and have high coercivity, which is important to the practical applications in ultrahigh density data storage media and magnetic nano devices.

Introduction

Nanoparticles of iron−platinum alloys have been under intensive study in recent years because of their magnetic properties.[1−8] There are three major different types of ordered FePt alloys, namely, Fe_3Pt, FePt, and $FePt_3$.[9] The face-centered tetragonal (fct) (also known as $L1_o$ phase) FePt alloy is particularly desirable because of its high magnetic anisotropy, high coercivity, small domain wall width (2.8−3.3 nm), small minimal stable grain sizes (2.9−3.5 nm), and chemical stability.[1,3] These properties make fct FePt nanoparticles excellent candidates and widely studied systems for applications in ultrahigh density magnetic storage media and for making advanced magnetic materials.[2−6,10]

Currently, monodisperse magnetic nanoparticles of FePt alloy are synthesized through the simultaneous reduction of metal salts and thermal decomposition of organometallic compounds in the presence of mixed surfactants.[5,8,11] The stabilizing agent is important for the formation of monodisperse FePt nanoparticles in the disordered face-centered cubic (fcc) phase.[5,8] The assembled nanoparticles can be converted into fct FePt alloys after annealing at enhanced temperatures. It is important to note that the monodisperse FePt nanoparticles made using wet chemistry methods typically have diameters in the size range of 4 to 6 nm.[5,8] For many practical applications, magnetic nanoparticles larger than 6 nm are preferred because coercivity H_c and remanence to saturation magnetization ratio M_r/M_s of the nanoparticles are closely related to the volume or size of magnetic nanoparticles.[12,13] These two properties have maximum values when the nanoparticles reach the critical sizes, which are around a few tens of nanometers in diameter depending on the chemical composition and crystalline structure of the particles. For instance, 20−40 nm nanoparticles have the highest coercivities for the CoNi alloy system.[12] Nanoparticles gradually become superparamagnetic due to random anisotropy when they are smaller than the critical size. Domain structure exists in particles larger than the critical size and is responsible for the decrease of coercivity and remanent magnetization. Unfortunately, the Ostwald ripening, which has been successfully applied to production of semiconductor quantum dots[14] and

† Department of Chemical Engineering.
‡ Laboratory for Laser Energetics.

(1) Weller, D.; Doerner, M. F. *Annu. Rev. Mater. Sci.* **2000**, *30*, 611−644.
(2) For recent developments in FePt nanostructures, see: *J. Appl. Phys*, **2003**, *93* (*10*), Part II.
(3) Weller, D.; Moser, A.; Folks, L.; Best, M. E.; Lee, W.; Toney, M. F.; Schwickert, M.; Thiele, J.-U.; Doerner, M. F. *IEEE Trans. Magn.* **2000**, *36*, 10−15.
(4) Skomski, R. *J. Phys.: Condens. Matter* **2003**, R841−R896.
(5) Sun, S. H.; Murray, C. B.; Weller, D.; Folks, L.; Moser, A. *Science* **2000**, *287*, 1989−1992.
(6) Zeng, H.; Li, J.; Liu, J. P.; Wang, Z. L.; Sun, S. H. *Nature* **2002**, *420*, 395−398.
(7) Sellmyer, D. J.; Luo, C. P.; Yan, M. L.; Liu, Y. *IEEE Trans. Magn.* **2001**, *37*, 1286−1291.
(8) Sun, S.; Anders, S.; Thomson, T.; Baglin, J. E. E.; Toney, M. F.; Hamann, H. F.; Murray, C. B.; Terris, B. D. *J. Phys. Chem. B* **2003**, *107*, 5419−5425.
(9) Wijin, H. P. J., Ed. *Magnetic Properties of Metals: d-Elements, Alloys and Compounds*; Springer-Verlag: Berlin, 1991.
(10) Redl, F. X.; Cho, K.-S.; Murray, C. B.; O'Brien, S. *Nature* **2003**, *423*, 968−971.
(11) Hyeon, T. *Chem. Commun.* **2003**, 927−934.
(12) (a) Toneguzzo, P.; Acher, O.; Rosenman, I. *IEEE Trans. Magn.* **1999**, *35*, 3469−3471. (b) Mercier, D.; Lévy, J.-C. S.; Viau, G.; Fiévet-Vincent, F.; Fiévet, F.; Toneguzzo, P.; Acher, O. *Phys. Rev. B* **2000**, *62*, 532−544.
(13) O'Handley, R. C. *Modern Magnetic Materials*: *Principle and Applications*; Wiley-Interscience Publication: New York, 2000; pp 434−437.
(14) Murray, C. B.; Kagan, C. R.; Bawendi, M. G. *Annu. Rev. Mater. Sci.* **2000**, *30*, 545−610.

silver nanowires[15] of various sizes does not seem to work on FePt nanoparticles. In this paper, we present a synthetic route to fct FePt nanoparticles and granular films using Pt@Fe_2O_3 core−shell nanoparticles as precursors through solid-state conversion. Using these core−shell nanoparticle precursors, we can make FePt magnetic nanoparticles not only with the preferred fct phase but also in a size range that has not been achievable using wet chemistry synthetic approaches.

Experimental Section

Synthesis of fct Phase FePt Nanoparticles and Granular Films from Pt@Fe_2O_3 Core−Shell Nanoparticles. In a standard preparation, Pt@Fe_2O_3 core−shell nanoparticles were made in octyl ether (2.5 mL) with a reactant mixture of platinum acetylacetonate (100 mg, 0.25 mmol), iron carbonyl ($Fe(CO)_5$, 55 μL, 0.4 mmol), oleic acid (80 μL, 0.6 mmol), oleylamine (80 μL, 0.6 mmol), and 1,2-hexadecanediol (0.2 g, 0.75 mmol) following the procedure described in the literature.[16] After the reaction, the core−shell nanoparticles went through several size selection cycles using ethanol and hexane.[5] These core−shell particles were then deposited as a monolayer on a substrate using a Langmuir−Blodgett system (Model KSV 3000) at a surface pressure of 45 mN m^{-1}. The Langmuir−Blodgett technique used in this work was the same as the one we used to deposit γ-Fe_2O_3 nanoparticles.[17] The solid-state conversions to the final FePt products were conducted at either 550 or 650 °C for 9 h under a flow of Ar(95%)/H_2(5%) gas in a tube furnace (Lindberg/Blue M, Model number TF55035A-1). The iron oxide shell was reduced to iron and formed the FePt alloy via solid-state reactions.[6] A procedure similar to that for making FePt nanoparticles was used to convert Pt@Fe_2O_3 core−shell nanoparticles into fct FePt films. In the latter case, a multilayered assembly, instead of the LB monolayer of Pt@Fe_2O_3 core−shell nanoparticles made by drop casting, was used.

Characterization. The transmission electron microscope (TEM) images and selected area electron diffraction (SAED) were recorded on a JEOL JEM 2000EX microscope at an accelerating voltage of 200 kV. A field-emission scanning electron microscope (FE-SEM; Model LEO 982) was used to study the surface of thin films. Energy-dispersive X-ray (EDX) analysis for FePt granular films was obtained with an EDAX detector installed on the same FE-SEM. The microscope was calibrated using Cu and Al element standards prior to the sample measurements. Composition analysis of individual FePt nanoparticles using EDX was done using an ultrahigh vacuum scanning transmission electron microscope (UHV-STEM) with an Oxford windowless Si(Li) detector equipped with a 4π pulse processor. This detector enables elemental identification down to boron, on areas as small as 1 nm^2 and with typically ~140 eV resolution. Powder X-ray diffraction (PXRD) spectra were recorded on a Philips MPD diffractometer with a Cu Kα X-ray source (λ = 1.5405 Å). The magnetic properties of the FePt films were determined using a Quantum Design AC and DC Superconducting QUantum Interference Device (AC/DC SQUID; Model MPMS XL) magnetometer. A specimen was typically made by drop-casting appropriate core−shell nanoparticles on a silicon wafer substrate followed by conversion to FePt alloys at the designed temperatures. Particle size analysis was conducted using Scion Imaging Software from Scion Corporation.

Results and Discussion

Scheme 1 is an illustration of the synthetic approach for making FePt nanoparticles from Pt@Fe_2O_3 core−shell nanoparticles. The reduction of iron oxide and the alloy formation of FePt can be accomplished at temperatures above ~450 °C in the presence of reducing gas and an inert atmosphere.[6] In our current approach, we use 5% hydrogen to reduce the iron oxide under the protection of argon at the reaction temperatures of 550 and 650 °C.

Scheme 1. Synthesis of FePt Nanoparticle from Pt@Fe_2O_3 Core−Shell Nanoparticle

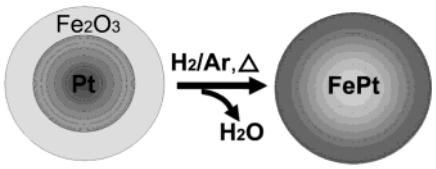

Platinum−iron oxide core−shell nanoparticles were made using a sequential deposition method we have developed.[16] Using this method, various thicknesses of the shell material could be deposited on Pt cores in a one-pot synthesis. Figure 1a shows bright field TEM images of core−shell particles that have Pt cores with an average diameter of ~10 nm and iron oxide shells of ~3.5 nm. Such a configuration was optimized for making FePt alloy. The cores and shells can clearly be distinguished because of the sharp contrast between iron and platinum due to their large difference in the electron penetration efficiency. Figure 1b shows the representative TEM image of FePt nanoparticles after the conversion at 550 °C on a thin amorphous carbon support. We used the LB deposition technique to control the monolayer arrangement of Pt@Fe_2O_3 core−shell nanoparticles on substrates. At a surface compression pressure of 45 mN m^{-1}, core−shell nanoparticles could form a densely packed and stable monolayer. Core−shell nanoparticles that spread using drop casting could form multilayered assembly and coalesce during the solid-state conversion to FePt alloy at the enhanced temperatures. The coalescence led to the broadening of the size distribution of FePt nanoparticles. The nanoparticles obtained using LB monolayers were uniform in size in large areas, Figure 1c. Figure 2 shows the particle size analysis for FePt nanoparticles using ~250 nanoparticles based on TEM images. The average diameter of these particles was 17.1 ± 1.2 nm, which agreed well with the overall diameter of those core−shell nanoparticles. To the best of our knowledge, uniform FePt nanoparticles of this size, either in fct or fcc phases, have not been made previously using colloidal synthetic methods.

Figure 3 shows the representative SAED pattern of a single layer of 17 nm FePt nanoparticles converted from Pt@Fe_2O_3 core−shell nanoparticles. The observed SAED patterns can be assigned to the fct FePt alloy (space group: *P*4/*mmm*, also see PXRD spectrum for the annealed multilayer assembly of FePt nanoparticles).[6] The electron diffraction rings of {002} and {200} planes in fct FePt nanoparticles are too close to be differentiated from each other, as are the rings for {220} and {202} planes. Relatively high crystallinity can be obtained for these nanoparticles, judging by the spotted electron diffraction patterns.

Granular films were formed through the transformation and coalescence of multilayered Pt@Fe_2O_3 core−shell nanoparticles. Figure 4 shows a representative SEM image of such a film made from assembly of Pt@Fe_2O_3 core−shell nanoparticles on a silicon wafer at 550 °C. The film showed the granular features due to the coalescence and sintering of FePt nanoparticles. It is

(15) Sun, Y.; Mayers, B.; Herricks, T.; Xia, Y. *Nano Lett.* **2003**, *3*, 955−960.
(16) Teng, X.; Black, D.; Watkins, N. J.; Gao, Y.; Yang, H. *Nano Lett.* **2003**, *3*, 261−264.
(17) Guo, Q.; Rahman, S.; Teng, X.; Yang, H. *J. Am. Chem. Soc.* **2003**, *125*, 630−631.

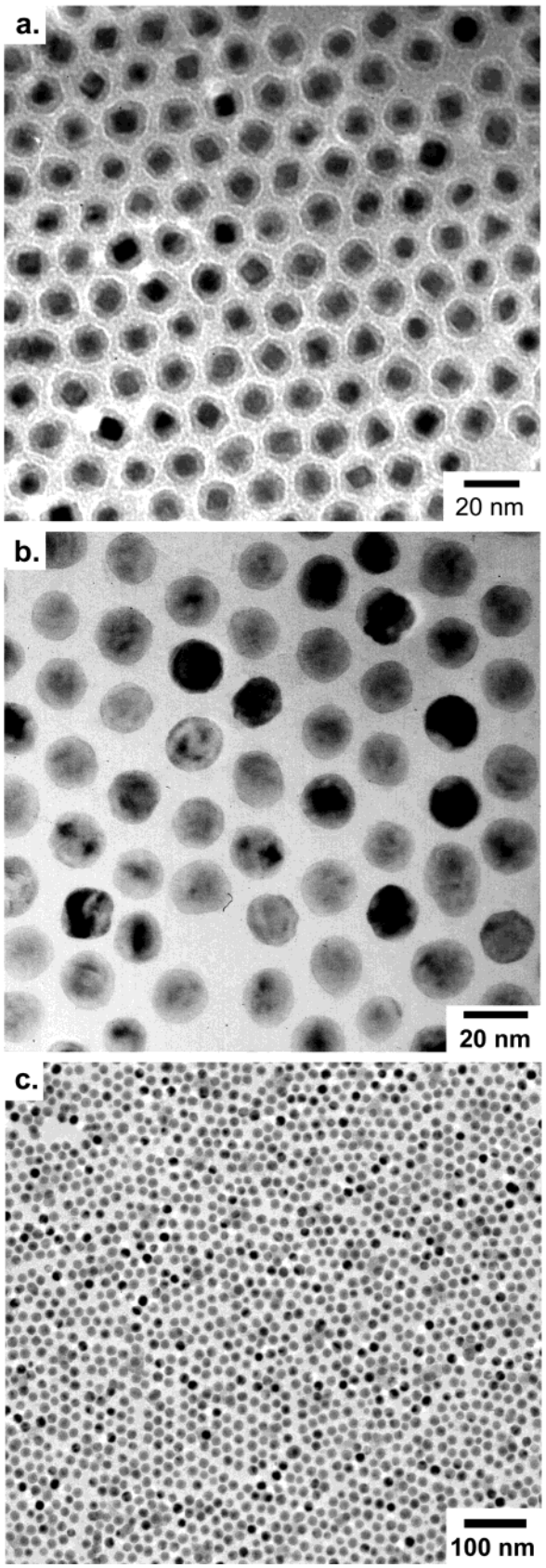

Figure 1. Bright field TEM images of monolayers of (a) Pt@Fe_2O_3 core−shell nanoparticles and (b, c) FePt nanoparticles.

feasible to improve the crystallinity of the films by controlling the packing density and order of the particles on the surface and the reaction temperatures.

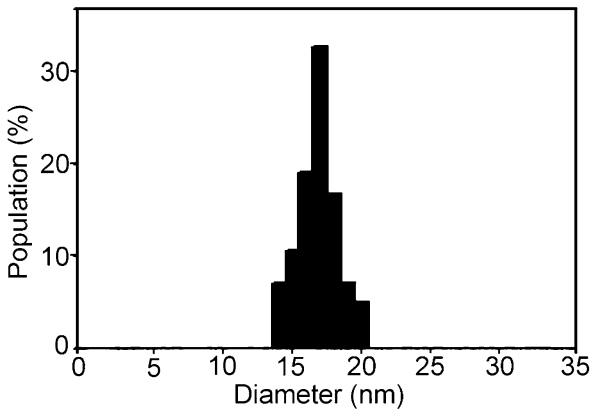

Figure 2. Particle size analysis of FePt nanoparticles.

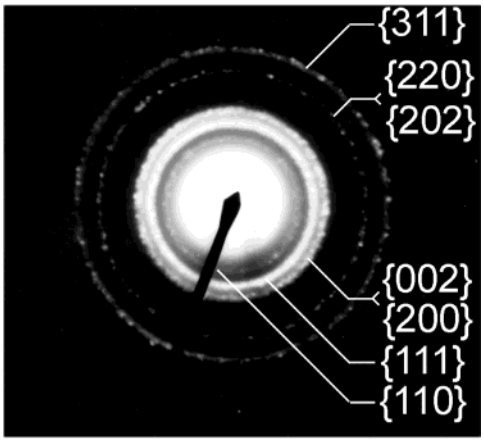

Figure 3. SAED of 17 nm FePt nanoparticles.

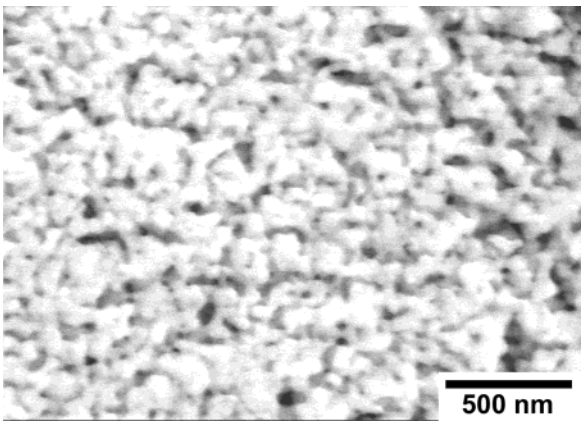

Figure 4. SEM image of an FePt granular film.

The elemental ratios of Fe to Pt in the FePt nanoparticles and granular films were characterized using EDX. The EDX data obtained based on the film samples should also represent the average Fe/Pt ratio of the FePt nanoparticles made from the same Pt@Fe_2O_3 core−shell nanoparticles. Figure 5 shows the EDX spectrum for the granular films made at 550 °C. Energy bands from both Fe (L line, 0.7 keV; K_α line, 6.4 keV; K_β line, 7.1 keV) and Pt ($M_{\alpha,\beta}$ lines, 2.1 keV; L_α line, 9.4 keV; L_β line, 11.1 keV) could be observed. We did the EDX analyses on various regions with a typical scan area of 3.6 μm^2 using different samples and consistently obtained an atomic ratio of $Fe_{56}Pt_{44}$. This ratio also represented the average atomic ratio of Fe to Pt in the FePt nanoparticles. Although they had uniform

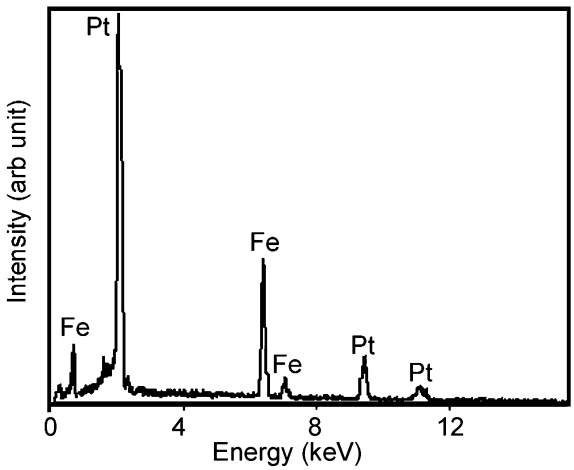

Figure 5. EDX analysis of the FePt granular film.

Table 1. Compositional Analysis of Eight Randomly Selected FePt Nanoparticles Using UHV-STEM

	weight percent (%)		atomic percent (%)	
particle no.	Pt	Fe	Pt	Fe
1	76	24	47	53
2	79	21	52	48
3	78	22	51	49
4	79	21	52	48
5	80	20	53	47
6	78	22	50	50
7	79	21	51	49
8	75	24	48	52

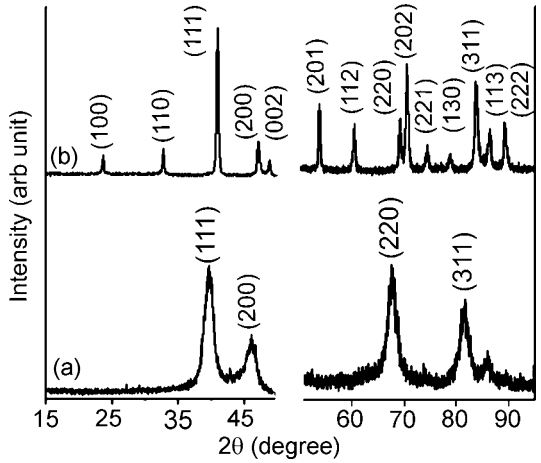

Figure 6. Powder XRD of (a) Pt@Fe_2O_3 core−shell nanoparticles and (b) fct FePt granular film made from these core−shell nanoparticle assemblies.

sizes when made from the Pt@Fe_2O_3 core−shell nanoparticles, the individual FePt nanoparticles could have slightly different Fe/Pt atomic ratios. Table 1 summarizes the results of EDX analysis on eight randomly selected FePt nanoparticles at the different grids of a specimen using the UHV-STEM. The atomic ratios of these eight nanoparticles varied around $Fe_{50}Pt_{50}$.

Figure 6 shows the representative PXRD spectra of the Pt@Fe_2O_3 core−shell nanoparticles and the FePt granular film made at 550 °C. The diffraction at 39.8°, 46.3°, 67.5°, and 81.3° 2θ shown in Figure 6a can be indexed to (111), (200), (220), and (311) planes of platinum in a cubic phase (space group: *Fm*3*m*), respectively (JCPDS database-International Centre for Diffraction Data, 1999, PCPDFWIN v. 2.02). The absence of

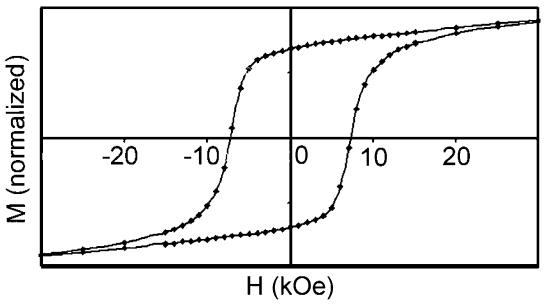

Figure 7. Hysteresis loop of a granular film of fct FePt alloy converted from a multilayered Pt@Fe_2O_3 nanoparticle assembly at 550 °C. The measurement was conducted at 5 K.

iron oxide diffractions was most likely due to the low crystallinity of the iron oxide and the heavy atom effect from platinum.[16] After conversion, these XRD peaks shifted to 41.1°, 47.1°, 68.9°, and 83.4° 2θ, and additional peaks could also be observed. These diffractions match very well with those from (002), (202), and other crystal planes of fct FePt alloy (space group: *P*4/*mmm*). The XRD peaks of the film samples were relatively narrow compared to those of Pt@Fe_2O_3 core−shell nanoparticles,[16] most likely because of the increased crystallinity and the coalescence of the nanoparticles during the reaction/sintering at 550 °C. The XRD trace for FePt films made at 650 °C was similar to that presented in Figure 6b. Our converging evidence from SAED, EDX, and PXRD analysis indicates that the final products were made of fct FePt alloys.

The fct FePt alloys have been shown to possess high coercivity after annealing at enhanced temperatures.[5,8,18,19] We have measured the magnetic properties of the FePt films made by the conversion of Pt@Fe_2O_3 core−shell nanoparticles at 550 °C using SQUID magnetometer. Figure 7 shows the hysteresis loop (normalized magnetization vs magnetic field, M/M_s-H curve) of an FePt film. This loop shows the characteristic of a ferromagnetic material. The coercivity of this film was 8.0 kOe measured at 5 K. It is known that FePt alloys can have various coercivities depending on the synthetic conditions, annealing temperatures, and compositions,[3,8,18,20−23] because coercivity is not an intrinsic property.[24] Our data agreed well with those of thin films of FePt alloys that were annealed under similar annealing temperatures.[3,19] We further examined the coercivity of the FePt granular films made from Pt@Fe_2O_3 core−shell nanoparticles at 650 °C. Figure 8 show the hysteresis loops ($M-H$ curves) of such FePt film specimen measured at 5 and 300 K. The coercivities were 9.1 kOe at 5 K and 7.0 kOe at 300 K. The coercivity increased when the reaction/annealing temperature increased in this range; a trend that agreed well with those observed previously.[5] Considering that no specific handlings and alignments in the synthetic steps were necessary

(18) Weller, D.; Sun, S. H.; Murray, C.; Folks, L.; Moser, A. *IEEE Trans. Magn.* **2001**, *37*, 2185−2187.
(19) Sun, S. H.; Fullerton, E. E.; Weller, D.; Murray, C. B. *IEEE Trans. Magn.* **2001**, *37*, 1239−1243.
(20) Vedantam, T. S.; Liu, J. P.; Zeng, H.; Sun, S. *J. Appl. Phys.* **2003**, *93*, 7184−7186.
(21) Ding, Y.; Yamamuro, S.; Farrell, D.; Majetich, S. A. *J. Appl. Phys.* **2003**, *93*, 7411−7413.
(22) Kang, S. S.; Nikles, D. E.; Harrell, J. W. *J. Appl. Phys.* **2003**, *93*, 7178−7180.
(23) Bo, B.; Laughlin, D. E.; Sato, K.; Hirotsu, Y. *IEEE Trans. Magn.* **2000**, *36*, 3021−3023.
(24) Givord, D.; Rossignol, M.; Bartherm, V. M. T. S. *J. Magn. Magn. Mater.* **2003**, *258*−*259*, 1−5.

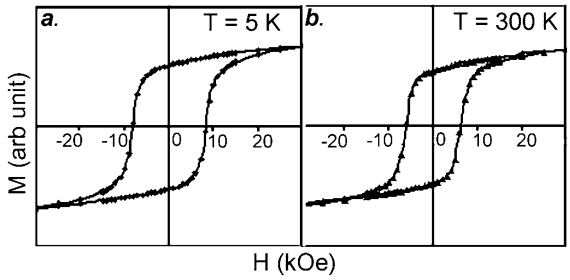

Figure 8. Hysteresis loops of a granular film of fct FePt alloy converted from a multilayered Pt@Fe_2O_3 nanoparticle assembly at 650 °C. The measurement was conducted at (a) 5 and (b) 300 K.

and the granular feature of these films, we believe the coercivities of these FePt alloys can be improved further.

Conclusions

We have presented a new method of making crystalline fct FePt nanoparticles and granular films from Pt@Fe_2O_3 core−shell nanoparticles. These fct FePt nanoparticles (17 nm in diameter) are in a size range that has not been synthesized using wet chemistry approaches. Such particles could be very useful in the study of magnetic properties at the mesoscopic range[25] and have broad ramifications in developing practical systems for data storage and in making solid-state magnetic nanodevices. This synthetic method can potentially be used to make FePt nanoparticles with different diameters, and other nanoparticles and thin films, such as CoPt and AgCo alloys from their corresponding core−shell particles.[26−30]

Acknowledgment. This work is partially supported by the University of Rochester and by the U.S. Department of Energy (DE-FC03-92SF19460). We are grateful to LLE for a Horton Fellowship (X.T). We thank Dr. Fangcheng Chou at MIT Center for Materials Science and Engineering (SQUID), Dr. Malcolm Thomas at Cornell Center for Materials Research (UHV-STEM), and Mr. Brian McIntyre (TEM) for their technical assistance. This work made use of the MSERC Shared Experimental Facilities supported by the National Science Foundation (DMR98-08941). The support of DOE does not constitute an endorsement by DOE of the views expressed in this article.

JA0376700

(25) Majetich, S. A.; Jin, Y. *Science* **1999**, *284*, 470−473.

(26) Liz-Marzan, L. M.; Correa-Duarte, M. A.; Pastoriza-Santos, I.; Mulvaney, P.; Ung, T.; Giersig, M.; Koyov, N. A. In *Handbook of Surfaces and Interfaces of Materials: Nanostructured Materials, Micelles, and Colloids*; Nalwa, H. S., Ed.; Academic Press: San Diego, 2001; Vol. 3, pp 189−237.

(27) Park, J. I.; Cheon, J. *J. Am. Chem. Soc.* **2001**, *123*, 5743−5746.

(28) Sobal, N. S.; Ebels, U.; Möhwald, H.; Giersig, M. *J. Phys. Chem. B* **2003**, *107*, 7351−7354.

(29) Sobal, N. S.; Hilgendorff, M.; Mohwald, H.; Giersig, M.; Spasova, M.; Radetic, T.; Farle, M. *Nano Lett.* **2002**, *2*, 621−624.

(30) O'Connor, C. J.; Sims, J. A.; Kumbhar, A.; Kolesnichenko, V. L.; Zhou, W. L.; Wiemann, J. A. *J. Magn. Magn. Mater.* **2001**, *226*, 1915−1917.